Natural and designed proteins inspired by extremotolerant organisms can form condensates and attenuate apoptosis in human cells

Mike T. Veling[1,2,7], Dan T. Nguyen[1,2,7], Nicole N. Thadani[1], Michela E. Oster[1,2], Nathan J. Rollins[1,2], Kelly P. Brock[1], Neville P. Bethel[3,4], David Baker[3,4,5], Jeffrey C. Way[1,2], Debora S. Marks[1,6], Roger L. Chang[1,2,8], Pamela A. Silver[1,2,8]

Affiliations

1. Department of Systems Biology, Harvard Medical School, Boston, MA, 02115, USA;
2. Wyss Institute for Biologically Inspired Engineering, Boston, MA, 02115, USA;
3. Institute for Protein Design, University of Washington, Seattle, WA, 98195, USA;
4. Department of Biochemistry, University of Washington, Seattle, WA, 98195, USA;
5. Howard Hughes Medical Institute, University of Washington, Seattle, WA, 98195, USA;
6. Broad Institute of Harvard and MIT, Cambridge, MA, 02142, USA;
7. Co-first authors
8. Co-corresponding authors

Key words

Stress tolerance, Phase separation, Intrinsically disordered proteins, Apoptosis

ABSTRACT

Many organisms can survive extreme conditions and successfully recover to normal life. This extremotolerant behavior has been attributed in part to repetitive, amphipathic, and intrinsically disordered proteins that are upregulated in the protected state. Here, we assemble a library of approximately 300 naturally-occurring and designed extremotolerance-associated proteins to assess their ability to protect human cells from chemically-induced apoptosis. We show that proteins from tardigrades, nematodes, and the Chinese giant salamander are apoptosis protective. Notably, we identify a region of the human ApoE protein with similarity to extremotolerance-associated proteins that also protects against apoptosis. This region mirrors the phase separation behavior seen with such proteins, like the tardigrade protein CAHS2. Moreover, we identify a synthetic protein, DHR81, that shares this combination of elevated phase separation propensity and apoptosis protection. Finally, we demonstrate that driving protective proteins into the condensate state increases apoptosis protection, and highlight the ability for DHR81 condensates to sequester caspase-7. Taken together, this work draws a link between extremotolerance-associated proteins, condensate formation, and designing human cellular protection.

INTRODUCTION

When exposed to extreme environmental stress, extremotolerance-associated (*ExTol*) organisms enter a state of reduced cellular metabolic activity that promotes survival in harsh conditions. This state has been shown to protect these organisms from high salinity, desiccation, and even the vacuum of outer space [1]. To acclimate to these conditions,

47 *ExTol* organisms significantly upregulate the production of protective metabolites, like
48 trehalose [2], as well as tolerance-conferring proteins [3], many of which are intrinsically
49 disordered proteins (*IDPs*) with repetitive sequence and predicted amphipathic helices.
50
51 While the mechanism of protection is unknown, one model suggests these proteins
52 mediate formation of a gel- or glass-like material state within an entire cell to protect it
53 from damage [3]. The model posits that such proteins promiscuously interact with
54 membranes and proteins, increasing intracellular viscosity and protecting vulnerable
55 structures [4-6] (Figure 1A Top). Such interactions would also work to prevent stress-
56 induced protein unfolding and protein aggregation [7]. An alternative model suggests that
57 these proteins form intracellular phase-separated membraneless compartments with
58 distinct physical parameters (referred to here as *condensates*) that partition key stress-
59 sensitive cellular components [8] (Figure 1A Bottom). Within these dense protein
60 structures, essential components are sequestered and protected from damage. The
61 models are not mutually exclusive; for example, in the case of desiccation tolerance,
62 continued dehydration could lead phase-separated compartments to fuse, comprise
63 much (if not all) of the cell, and promote a glassy material state.

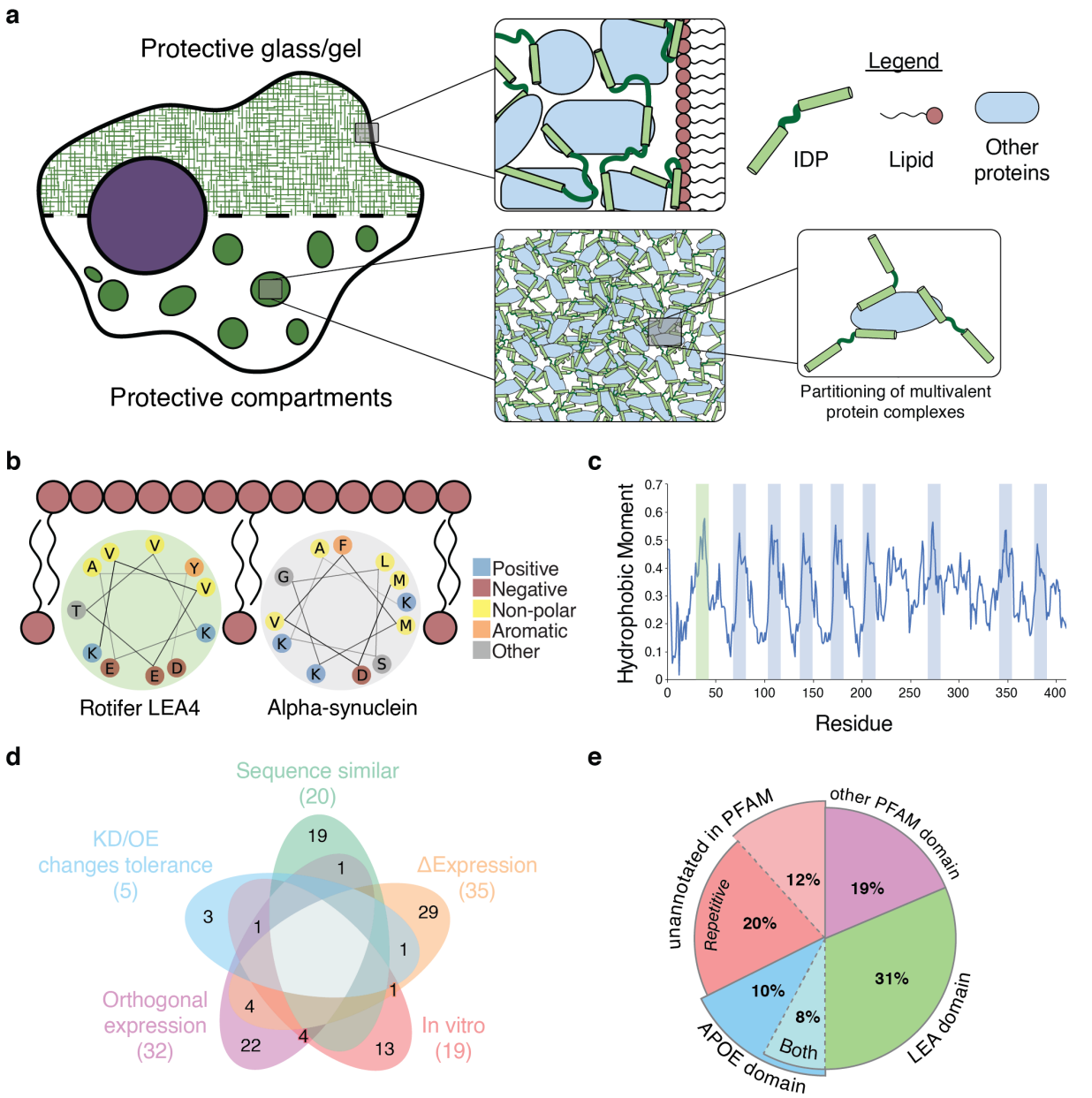

Figure 1: Selection of candidate extremotolerance-associated proteins (a) Illustration of different protective models for cellular stress tolerance. **(b)** Illustration of amphipathic membrane interaction for rotifer LEA4 protein and Alpha-synuclein, thus highlighting a feature indicative of extremotolerance-associated proteins. **(c)** Hydrophobic moment analysis of rotifer LEA4, showing the repetitive nature of the amphipathic signature. Highlighted green segment corresponds to the LEA4 helix in (b). **(d)** Venn diagram of the lines of evidence used to select targets in the final library. Abbreviations: KD, knockdown; OE, overexpression; Δ, change in expression levels. **(e)** Domain analysis of included targets reveals LEA and ApoE domains in almost half of the targets tested. The other half contains proteins with other PFAM domains (19%) or without any affiliated PFAM entry (32%). Of the proteins lacking a known PFAM annotation, many exhibit repetitive sequence (20% of all targets).

65

66 The resurgence of interest in biological phase separation, extensively reviewed in [9-12],
67 has shown that human cells can employ similar strategies to survive stressful conditions.
68 While the reversible formation of stress granules in healthy cells is the archetype of stress
69 tolerance, recent studies have revealed phase separation as a key adaptation that cancer
70 cells use to avoid apoptosis and cell death [13-14]. Phase-separated condensates have been
71 implicated in sequestering key tumor repressors[14], enhancing or repressing gene
72 expression in response to stress [15], and regulating mRNA or protein function through
73 sequestration [16]. These processes parallel the mechanisms that ExTol proteins are
74 thought to use to protect complex biological systems, suggesting there could be some
75 functional overlap. That is, sequence features and properties within ExTol proteins could
76 be implicated in mammalian stress tolerance pathways, including apoptosis resistance.

77

78 A key sequence feature of some ExTol proteins is the presence of amphipathic helices
79 [17]. While disordered in most contexts, ExTol proteins can transiently form amphipathic
80 helices in certain molecular environments, notably when interacting with and stabilizing
81 membranes [6]. The helices often exhibit a hydrophobic face, which interacts with core
82 lipids within the membrane, flanked by positively charged residues that might interact with
83 the negatively charged lipid head groups (Figure 1B). This amphipathic moment often
84 repeats across the length of the protein (Figure 1C). This feature is a hallmark of the late
85 embryonic abundant (LEA) class of ExTol proteins [18]. Human membrane interacting
86 proteins, like alpha-synuclein, also exhibit a similar repeat motif [19]. Such parallels in

87 sequence features suggest that orthogonal expression of ExTol proteins may confer their
88 protective properties to other biological systems, like human cells.
89
90 Indeed, previous reports have shown that some of these ExTol proteins provide similar
91 protective properties when expressed heterologously. Expressing tardigrade-specific
92 IDPs (TDPs) in bacteria provides protection against desiccation [3]. Anhydrin, an IDP
93 upregulated by *Aphelenchus avenae* during dehydration, expressed in a human cell line
94 limited PABPN1-A17 aggregation, a hallmark of oculopharyngeal muscular dystrophy [7].
95 Similar reports demonstrated protection of human cells provided by expression of LEA
96 proteins originating from the African midge [20] and by TDPs from tardigrades [21]. These
97 findings reinforce the promise of transferring protective phenotypes from their native
98 contexts to human cells.
99
100 Taken together, these data indicate a potential avenue for using this class of proteins to
101 protect biological systems in a controlled manner. To test this hypothesis, we generated
102 approximately 300 sequences inspired by ExTol proteins and examined their ability to
103 protect against apoptotic cell death. Our results show that human proteins containing
104 sequence hallmarks of ExTol proteins as well as *de novo* designed condensate forming
105 proteins can protect human cells from chemically-induced apoptosis. We also
106 demonstrate that condensate induction using synthetic modifications can strengthen
107 apoptotic protection. Finally, we show that key components of the apoptotic pathway can
108 localize to inducible condensates, suggesting enzyme sequestration could be a
109 mechanism of action.

110

111 **RESULTS**

112 **Assembling a library of stress tolerance proteins**

113 Based on the hallmark sequence features of ExTol proteins, we searched the published
114 literature to identify proteins that not only contain these features but also exhibit some
115 evidence for protection of biological structures. The library was generated based on over
116 one hundred naturally-occurring proteins based on five lines of evidence for stress
117 tolerance association, including: change in expression during extremotolerance,
118 knockdown or overexpression changing the tolerant state, *in vitro* protection, orthogonal
119 expression transferring tolerance, and sequence similarity to other proteins with these
120 features (Figure 1D and Supplemental table 1).

121

122 A PFAM domain analysis of the identified proteins reveals almost half of the identified
123 targets have two key domains: Late Embryonic Abundant (LEA) and Apolipoprotein E
124 (ApoE) domains (Figure 1E, Supplemental table 1). LEA proteins are well known to be
125 upregulated during the last stages of plant seed maturation [22]. This domain is thought to
126 protect the seed embryo during transport to its new destination. There is also evidence
127 that this domain has been co-opted by bacteria as protection from desiccation and
128 radiation [23]. ApoE proteins interact with lipid particles to allow for lipid reuptake into cells.
129 Additionally, mutations within human ApoE have been identified as strong genetic
130 predictors of Alzheimer's disease in human populations [24]. Based on their lipid interaction
131 properties and potential role in neuronal homeostasis, as well as its prevalence in the

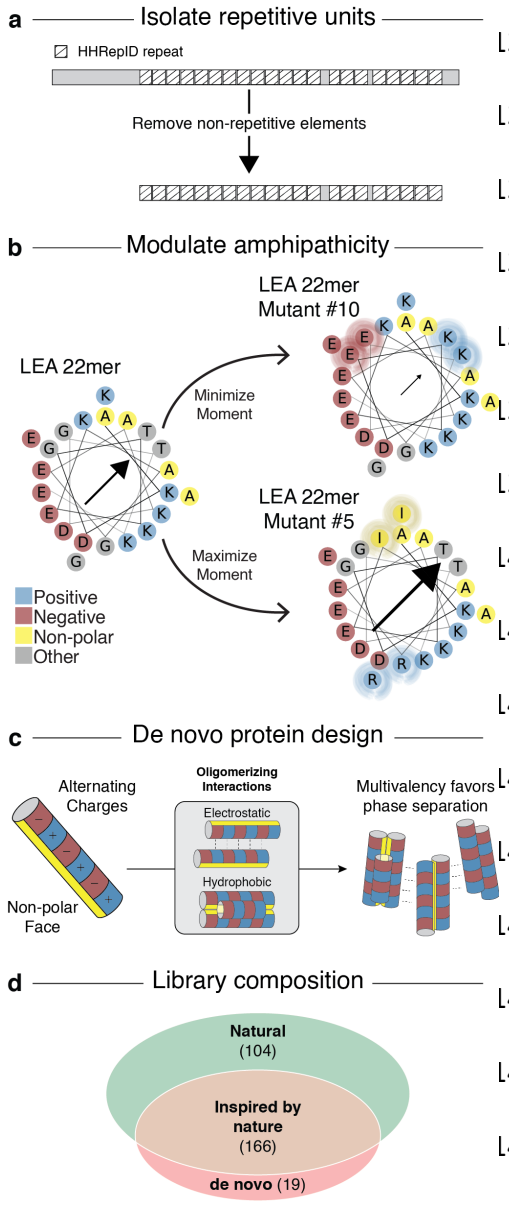

Figure 2: Design based on candidate extremotolerance-associated proteins. (a) Truncations were made to isolate regions of repetitive and amphipathic sequence. **(b)** Small helices were selected and altered based on their hydrophobic moment. **(c)** Synthetic alpha helix-containing proteins designed to oligomerize. **(d)** Venn diagram highlighting the library that was tested.

PFAM domain analysis, we decided to include human ApoE and its various mutations as ExTol proteins in our study.

Designing novel extremotolerance-associated proteins

To test hypotheses about sequence features and their relationship to phase separation and apoptosis, we designed novel proteins based on the set of ExTol proteins. These new designs take 3 approaches (Figure 2): truncation of proteins to focus on repetitive, intrinsically disordered, and amphipathic regions; isolation of individual helices with desired sequence features; and *de novo* design of alpha helix-containing proteins that self-assemble into higher order structures. Through these designs, we sought to identify the minimal elements required for protection and phase separation.

First, we identified regions within natural proteins that contain intrinsic disorder [25],

155 repetitive sequences [26], and amphipathic helices[27]. Figure 2A illustrates the use of
156 HHRepID on the sequence of full length human ApoE. Based on this analysis, we
157 identified the repeating domain within ApoE for further testing. Other ExTol proteins were
158 similarly modified and examined.
159
160 We also included short peptides based on the consensus sequence of repetitive regions
161 that have previously been shown to be protective [28]. To test if any of the sequence
162 features we identified are important for apoptosis protection, we altered these features
163 within these short peptides. For example, we altered the amphipathic character of these
164 helices (Figure 2B) to determine if apoptosis protection was changed.
165
166 To examine whether generic condensate formation is sufficient to confer apoptosis
167 protection, we also examined completely synthetic alpha helix-containing proteins that
168 were designed to form repetitive structure with sequences orthogonal to naturally-
169 occurring proteins [29]. These designed helical repeat (DHR) proteins interact along the
170 axis of the helix, forming long spiraling fibrils, but may also potentially self-interact along
171 the face of the protein based on a pattern of positive and negative charges (Figure 2C).
172 This ability to oligomerize and form multivalent complexes, which may then interact via
173 weak non-covalent interactions, is an established determinant of condensate formation
174 [12].
175
176 Together, our library consists of 104 naturally-occurring proteins, 166 truncations or
177 isolations of helical regions, and 19 *de novo* designs (Figure 2D). Taken altogether, these

178 proteins interrogate several hypotheses about how disordered proteins may protect
179 human cells against apoptosis.
180
181 **Apoptosis assay identifies extremotolerance-associated proteins in human cells**
182 To model stress in a mammalian cell system, we induced cellular apoptosis by treatment
183 with the chemotherapeutic camptothecin (CPT), a DNA topoisomerase inhibitor well
184 known to trigger apoptosis [30-31]. Under these conditions, protection against apoptosis
185 could be achieved through a number of avenues, including protection against the DNA
186 damage caused by CPT-induced topoisomerase inhibition [30], interruption of the signaling
187 cascade, or even protection of the mitochondrial membrane whose rupture ultimately
188 triggers apoptosis [32].
189
190 To test our designs for protection against apoptosis, we used a human cell-based
191 apoptosis assay (Figure 3A). This assay uses HT-1080 fibrosarcoma cells from ATCC [33].
192 These cells are seeded in a 96-well plate and allowed to adhere overnight. The next day,
193 the cells are co-transfected with a plasmid containing the ExTol candidate proteins of
194 interest as well as a transfection marker. The following day, the media is swapped to one
195 containing 13.2 μM CPT. After addition of CPT, caspase-3 and -7 activation is measured
196 by microscopy every 45 minutes for 1 day using a fluorophore quencher pair attached to
197 either end of a peptide with the sequence “DEVD”. As caspase-3 and -7 are activated,
198 the DEVD peptide is cleaved, releasing the fluorophore from the quencher. The
199 unquenched fluorophore localizes to the nucleus where it can be quantified by imaging
200 on a single-cell level. The single-cell resolution allows for the separation of transfected

201 and non-transfected cells based on the transfection marker. Only single cells with the
202 transfection marker were subjected to further analysis; Figure 3B shows sample images
203 highlighting the type of data being analyzed.
204
205 On every plate, an empty vector negative control is run as well as a positive control
206 containing the X-linked inhibitor of apoptosis (XIAP). This protein is known to bind to
207 caspase-3 and -7 to block their activity [34] . Figure 3C shows example data comparing
208 median DEVD peptide signal intensity over time after induction with CPT of four wells on
209 the same plate transfected with XIAP and empty vector. The results show a reduction in
210 DEVD peptide signal intensity when the XIAP-containing vector is transfected,
211 demonstrating that the assay can identify modulators of apoptosis.
212
213 To convert these time-resolved data to a measure of protection against apoptosis, the
214 maximum DEVD peptide signal intensity is calculated and normalized to a plate-matched
215 empty vector control (see methods for further details). The normalized apoptosis induction
216 intensity is shown in Figure 3D left. The data are slightly skewed towards apoptosis-
217 protection, which supports our hypothesis that the targeted proteins can protect against
218 apoptosis.
219

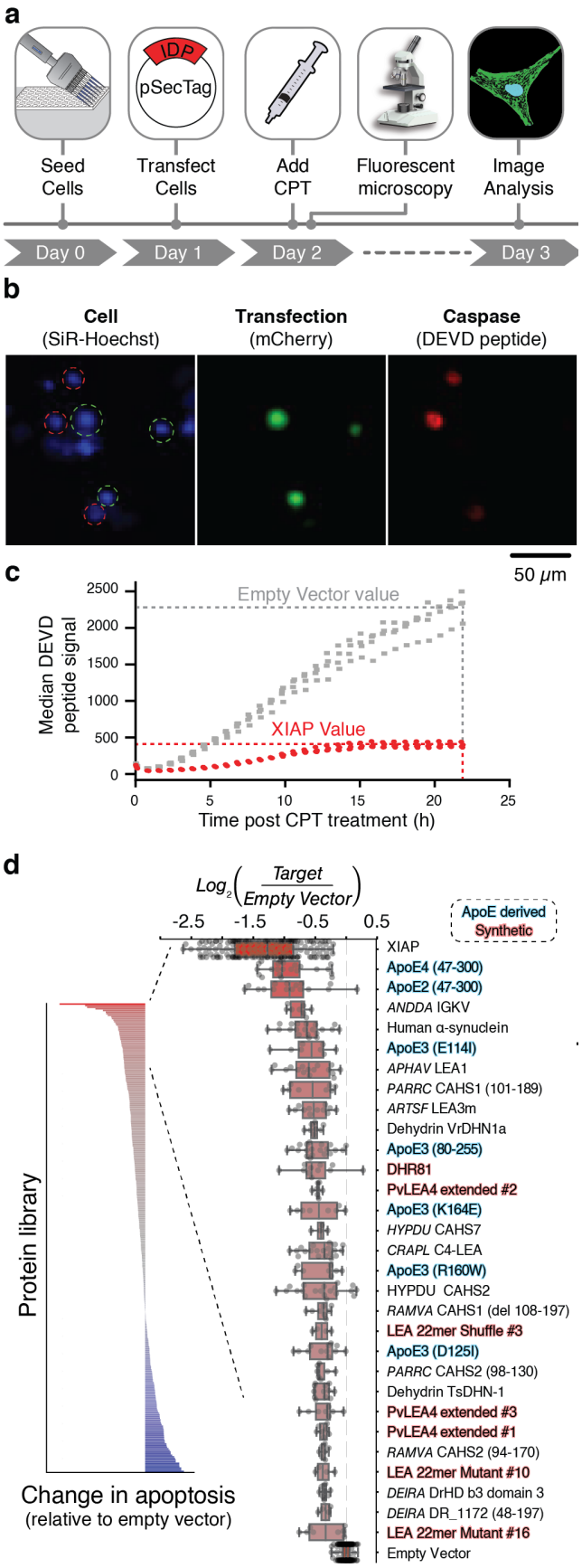

Figure 3: Screen for CPT resistance by extremotolerance-associated proteins (a) Flow diagram of the assay. **(b)** Representative images showing cells during the assay. Cells are identified using SiR-Hoechst marking the nucleus (*blue*). Transfected cells are identified by the presence of the mCherry marker (*green*). Finally, the degree of apoptosis is identified by the presence of the cleaved DEVD peptide (*red*). **(c)** Positive control showing apoptosis reduction upon expression of XIAP. **(d)** Bar graph highlighting the apoptosis resistance provided by different constructs, including zoomed in area to highlight the top hits in the assay. Source species of a sequence are abbreviated and shown in italics; abbreviations are drawn from Uniprot, including *RAMVA* (*Ramazzottius varieornatus*), *HYPDU* (*Hypsibius dujardini*), *PARRC* (Paramacrobiotus richtersi), *ANDDA* (*Andrias davidianus*), *APHAV* (*Aphelenchus avenae*), *ARTSF* (*Artemia franciscana*), *CRAPL* (*Craterostigma plantagineum*), and *DEIRA* (*Deinococcus radiodurans*).

220

221

222 To highlight the top-performing designs, the top 10% of the targets are shown in Figure
223 3D right. As expected, the XIAP positive control showed the strongest anti-apoptotic
224 effect. The two top-performing hits were ApoE designs. Human alpha-synuclein is the 5th
225 hit, which is expected as it is known to be both intrinsically disordered, and anti-apoptotic
226 [35]. Additionally, several ApoE designs and short LEA helices are top hits. The data used
227 to generate these figures is included in supplemental table 2.

228

229 **Known extremotolerance-associated proteins affect apoptosis**

230 Among the top hits in apoptosis reduction are an IGKV protein highly expressed in mucus
231 of the Chinese giant salamander *Andrias davidianus* [36] that is used as a medical glue in
232 traditional Chinese medicine, an LEA protein from the nematode *Aphelenchus avenae*
233 previously shown to have the ability to reduce a form of protein aggregation associated
234 with oculopharyngeal muscular dystrophy in human cells [7], and a mitochondrial LEA
235 protein from the brine shrimp *Artemia franciscana* shown to protect human cells during
236 desiccation [20] (Figure 3D). The prominence of these ExTol proteins suggests the assay
237 can help identify other proteins that can protect cells from more general stresses beyond
238 CPT-induced apoptosis.

239

240 **Short repetitive peptides and *de novo* designs modulate apoptosis**

241 LEA repeat-containing peptides are among the top-performing hits in the screen. While
242 the original short LEA designs from Furuki et al. 2019 had a minor effect reducing
243 apoptosis, several of the designs tested here performed better (Supplemental Figure 3A)

244 [28]. As 22 amino acids is small and could lead to peptide stability issues, longer 50-amino
245 acid designs inspired by the same LEA proteins Furuki et al. utilized were also developed
246 (Supplemental Figure 3B). Some of these designs were also able to reduce apoptosis,
247 including the PvLEA4 with extended repeats (notably PvLEA4 repeats extended #2),
248 which fell into the top hits of the entire library (Figure 3D and Supplemental Figure 3B).
249 These results suggest that optimization of synthetic designs yields proteins with stronger
250 function than naturally-occurring proteins.
251
252 While these proteins were designed to interrogate the relationship between sequence
253 and apoptosis protection in short peptides, little relationship was found with respect to the
254 sequence features we analyzed (Supplemental Figure 3C). Several designs were made
255 that would alter the hydrophobic moments of putative helices these peptides are predicted
256 to form. To examine if this sequence property relates to the stress-tolerance function of
257 these proteins, we attempted to correlate this property with assay performance. However,
258 no significant correlation was found, suggesting (at least in these cases) that degree of
259 amphipathicity on its own is not the key determinant of stress-tolerance function of these
260 proteins.
261
262 **The repeat region of ApoE comprises its minimal anti-apoptotic unit**
263 The top two hits in the assay were ApoE4 (47-300) and ApoE2 (47-300). These truncated
264 forms of ApoE maintain the repeat domains shown in Figure 4A, while removing the signal
265 peptide and terminal regions. This suggests that the repeat region of ApoE accounts for
266 its core anti-apoptotic functionality. Interestingly, the full length ApoE2 and E4 do not

267 show up as top hits, suggesting that these truncated forms improve on the apoptosis
268 protection provided by the full-length variants (Figure 4B).
269
270 Based on the location of the signal peptide, it is expected that ApoE4 should localize to
271 the secretory pathway whereas the truncated form may be cytoplasmic. To test this
272 hypothesis, cells were subjected to Western blot and immunofluorescence analysis using
273 commercially available antibodies (Abcam ab24139; Figure 4C and Supplemental Figure
274 4A). The Western blot results show that both the full-length and truncated forms of ApoE4
275 are expressed at the expected size (Supplemental Figure 4A). The immunofluorescence
276 shows co-localization between the ApoE4 full length protein and the endoplasmic
277 reticulum (marked by Thermo's PDI antibody MA3-019, Figure 4C). However, the
278 truncated form did not show the same co-localization, suggesting as expected that it may
279 not enter the secretory pathway as the full-length version does.
280
281 Strikingly, the truncated version appeared to form more pronounced puncta throughout
282 the cytoplasm of the cell, suggesting the formation of potentially phase-separated
283 condensates. In screening through the point mutants of ApoE also tested here, we found
284 a similar condensate phenotype with the full length ApoE3 D125I mutation (Supplemental
285 Figure 4B). Together, these data suggest that ApoE may be able to support condensate
286 formation and confer apoptosis protection in part via the protective compartment
287 mechanism (Figure 1A bottom).
288
289

290

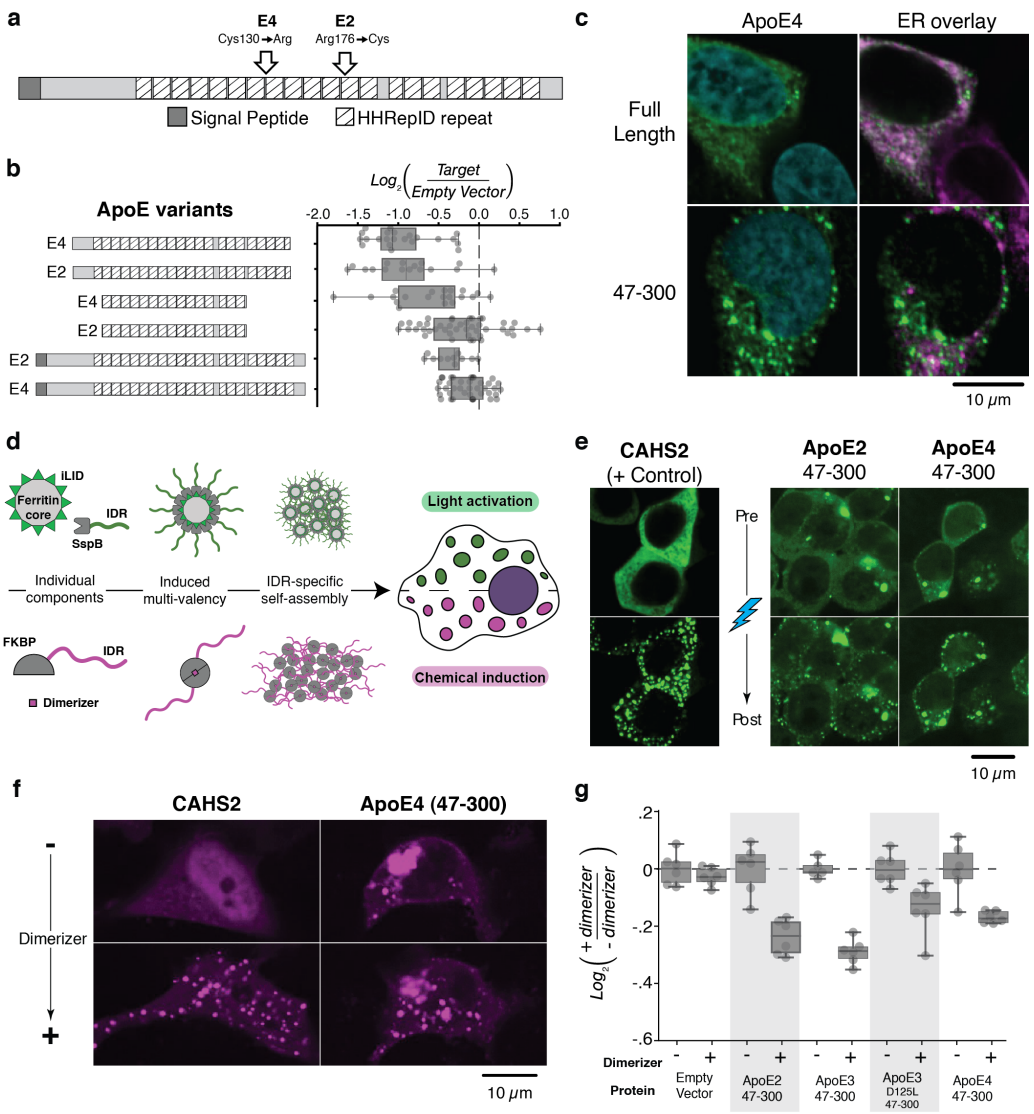

Fig. 4. ApoE truncations and synthetic condensates further reduce apoptosis.
(a) Gene diagram highlighting the repetitive region of ApoE. **(b)** Boxplots highlighting the apoptosis assay performance of the full length and truncated forms of ApoE2 and E4. **(c)** Immunofluorescence of ApoE4, full length and truncated forms. *White* indicates colocalization, which is more apparent with the full-length protein. The truncated form appears to exhibit larger and more distinguishable puncta. **(d)** Diagram of the induced multi-valency systems used here, including the light-inducible system (*top*) and the chemically-inducible system (*bottom*). **(e)** Condensate formation assay using the light-inducible system, including the CAHS2 positive control showing condensates only upon light induction and several ApoE examples that form condensates both before and after induction. **(f)** Condensate formation assay using the chemically-inducible system, including the CAHS2 positive control showing condensates only upon added dimerizer and ApoE4 (47-300) exhibiting condensates both before and after induction. **(g)** Apoptosis data showing reduction in apoptosis upon condensate induction with dimerizer. Data are normalized to mean apoptosis level of uninduced (i.e. no dimerizer) sample for each construct.

291 **CAHS2 and ApoE form condensates upon induced multivalency**

292 Established condensate engineering tools [37] were used to test for latent phase separation
293 propensity within the top performing proteins. We used both light- and chemically-
294 inducible systems of multivalency. In the light system, a ferritin core (comprised of self-
295 assembled monomers, FTH1 domain-eGFP-iLID) becomes decorated with SspB-
296 modified proteins upon exposure to blue light [38] (Figure 4D top). In the chemical system,
297 multivalency (i.e. multiple arms of the ExTol protein of interest) is induced using a
298 dimerization agent [39] that brings together FKBP-modified proteins [37] (Figure 4D bottom).
299 These inducible methods increase the valency of a system, and thus work to favor phase
300 separation. In this way, they can help reveal any latent ability to form condensates that is
301 not immediately observable without modification.

302

303 Indeed, condensates were observed in both inducible systems using ExTol proteins.
304 CAHS2, a protein from the tardigrade *P. richtersi*, exhibited the most dramatic phenotype,
305 which is consistent with recent work describing the gel forming capabilities of CAHS
306 proteins [40] (Figure 4E&F). ApoE variants were of particular interest, based on the puncta
307 observed in the top performing ApoE constructs. All versions of ApoE tested formed
308 puncta without activation, consistent with our previous observation using untagged native
309 ApoE (Figure 4C). Upon light- or chemical-activation, there is a noticeable increase in
310 condensates, exemplifying how phase separation can be enhanced with increased
311 multivalency (Figure 4E&F).

312

313 **Induction of condensates reduces apoptosis**

314 Induction of multivalency in ApoE containing constructs reduces apoptosis. We performed
315 the apoptosis assay using the top hits modified for chemically-induced multivalency,
316 namely fusion to two FKBP domains. The results show that the presence of the chemical
317 dimerizer did not affect apoptosis signal in cells transfected with the empty vector; in
318 contrast, the ApoE constructs exhibit reduced apoptosis with added dimerizer (Figure
319 4G). That is, artificially increasing ApoE condensates was apoptosis protective. These
320 data suggest that condensate formation plays a role in the anti-apoptotic effect of these
321 proteins.
322
323 **Synthetic DHR81 condensates reduce apoptosis and sequester caspase-7**
324 Induction of DHR81 based condensates protects against apoptosis. DHR81 is formed
325 from four helical hairpin repeat regions; the core of the protein is hydrophobic to ensure
326 consistent folding, while the outside of the protein is decorated with checkerboard positive
327 and negative charges (Figure 5A) [29]. This structure ensures the protein is well folded,
328 while also enabling the potential for higher order structure formation via electrostatic
329 interactions. Indeed, as with the ApoE variants, DHR81 supported condensates in the
330 chemically-inducible condensate system (Figure 5B) and exhibited a stronger anti-
331 apoptotic phenotype when multivalency is induced (Figure 5C and Supplemental Figure
332 5A). There was little to no effect in cells containing an empty vector or expressing the
333 FKBP dimerization domains alone.
334
335
336

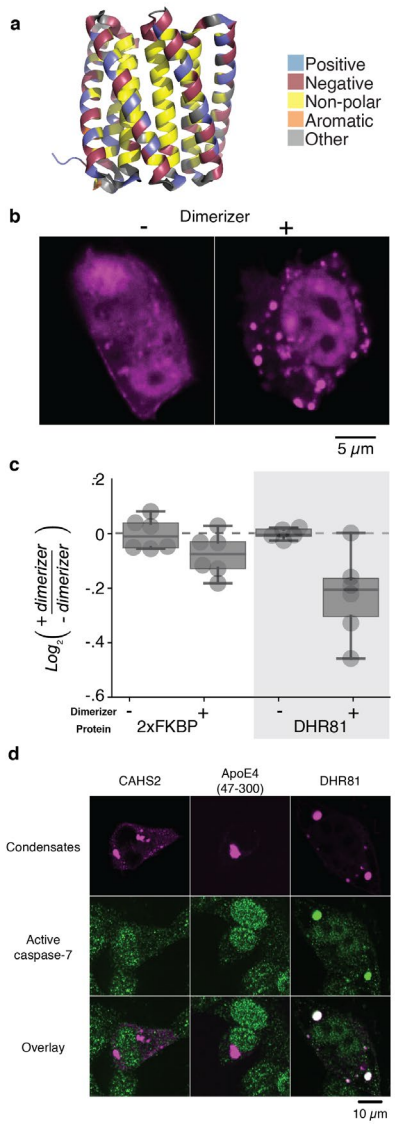

Fig. 5. DHR81 condensate formation and apoptosis reduction. (a) Diagram of DHR81, illustrating a charge distribution that can support oligomerization. **(b)** Sample images highlighting how the synthetic protein DHR81 supports chemically-induced condensates. **(c)** Apoptosis is further reduced in the presence of dimerizer (i.e. with induced DHR81 condensates). The FKBP-modifications alone, which enable chemically-induced multi-valency, have a minimal effect on apoptosis. **(d)** Activated caspase-7 (*green*) co-localizes with DHR81 condensates but not CAHS2 or ApoE4 (47-300) condensates (*magenta*). *White* indicates colocalization.

To further explore how condensates mediated by ExTol proteins may confer an anti-apoptotic effect, we examined whether they sequester major components of apoptotic signaling, namely caspase-3 and -7. The results showed that activated caspase-7 localized to DHR81 condensates but not CAHS2 or ApoE4 condensates (Figure 5D). Caspase-3, however, does not localize to either DHR81, CAHS2, or ApoE4 condensates (Supplemental Figure 5B). These results suggest sequestration of key apoptotic factors could be a mechanism by which these condensates reduce apoptosis.

Discussion

To broadly evaluate the ability of ExTol proteins to protect orthogonal systems from environmental stress, we studied over one hundred different ExTol proteins. We used these as a basis to design approximately 300 variants, including truncations and fusion proteins. These designs

360 were evaluated on their ability to protect human HT-1080 cells against CPT-induced
361 apoptosis. The results showed that known ExTol proteins, ApoE variants, and the
362 synthetic DHR81 protein could modulate apoptosis levels when transferred to human
363 cells.
364
365 Protection against apoptosis is a key feature of many ExTol proteins. As apoptosis is a
366 common cellular response to stress, the ability to mitigate this response is important in
367 providing cell-autonomous protection in stressful environments. While the mechanism
368 resilient organisms use to survive is still not fully understood, it is becoming increasingly
369 clear that phase separation may play an important role.
370
371 ExTol proteins are proposed to form expansive higher order structures (e.g. gels or glassy
372 systems) that reduce the viscosity of the cytoplasm, especially in desiccated states [3].
373 Other reports show that these proteins could mediate formation of protective phase-
374 separated compartments (i.e. condensates), sequestering damage-inducing proteins
375 and/or protecting important targets [8]. Based on our condensate data, it appears the latter
376 may be at play for proteins like ApoE or DHR81. Notably, in these proteins that already
377 exhibit both anti-apoptotic effects as well as elevated phase separation propensities,
378 increasing the amount of condensates via an engineered inducible system improved
379 protection against apoptosis. This observation suggests that condensates could be a key
380 part of the protective mechanism.
381

382 Interestingly, we observed that activated caspase-7 partitions into DHR81 condensates,
383 suggesting caspase sequestration as a potential anti-apoptotic mechanism. Phase-
384 separated condensates and higher order assemblies are already implicated in mediating
385 apoptosis: stress granules inhibit apoptosis by suppressing MAPK pathways [41]; the
386 apoptosome relies on Apaf-1 multimerization, which has been reported to undergo
387 amyloid fibrillation in specific conditions [42]; and stress-dependent phase separation
388 modulates proteasome formation, whose function affects apoptosis [43-44]. It is interesting
389 to note that we only observe clear caspase-7 partitioning into DHR81 condensates,
390 suggesting the possibility of a specific binding interaction in this case. ApoE condensates
391 may be sequestering other apoptotic factors or using a different mechanism to reduce
392 apoptosis.
393
394 It is also possible that these ExTol proteins achieve their anti-apoptotic effect by
395 implementing a more general physical mechanism, namely slowing the intracellular
396 mobility of biological effectors. There are various reports describing how the effective
397 viscosity within the cytoplasm can be increased in response to external stresses [4-5] or
398 mediated by protein composition, specifically intrinsically disordered proteins [45]. Notably,
399 a pervasive cell-spanning gel or network is not necessary to achieve such an effect; it is
400 possible that the presence of condensates, coupled with their ability to selectively partition
401 biomolecules (i.e. control what biomolecules can enter and diffuse through them), could
402 broadly slow biomolecular movement. That is, by forcing different proteins to either be
403 trapped in them or diffuse around them, condensates can decrease protein mobility and
404 perturb e.g. signaling pathways. Our results showing a lack of caspase-7 sequestration

405 by some of our protein condensates could thus support this more general mechanism of
406 condensates perturbing biology.
407
408 Condensates are becoming increasingly implicated in disease [10], particularly when their
409 structural metastability and reversibility is dysregulated (e.g. through mutation). Notably,
410 drugs that block the formation of amyloid fibrils and plaques, which are products of phase
411 separation dysregulation, are promising yet strongly debated [46] therapies for many
412 neurological diseases. As such, our observations of ApoE are particularly salient. We
413 found that expression of a cytoplasmic form of ApoE is protective against apoptosis. In
414 particular, the truncated repeat region of ApoE is sufficient and shows the strongest anti-
415 apoptotic activity of all designs we tested. Others have shown similar effects for
416 exogenously added ApoE-containing liposomes protecting rat neurons against apoptosis
417 [47], though we show the effect through overexpression of ApoE inside of human cells.
418 When combined with our condensate results and the clinical relevance of ApoE in
419 Alzheimer's disease [48], these observations suggest the anti-apoptotic effect observed
420 here warrants further study, to further elucidate its role in Alzheimer's disease
421 progression.
422
423 Altogether, our work expands upon the understanding of the relationship between
424 condensate formation and cell physiology, demonstrating how condensate accumulation
425 can be broadly beneficial in reducing apoptosis while also identifying diverse new protein
426 domains that confer protection. The proteins and concepts presented here demonstrate

427 the utility of this class of proteins for engineering new properties into cells and ultimately
428 higher organisms.
429
430 **Methods**
431 **Cell culturing and maintenance**
432 HT-1080 cells (ATCC, CCL-121) were maintained in EMEM medium supplemented with
433 10% FBS and Penicillin-Streptomycin according to ATCC's protocol. For additional details
434 see supplemental methods.
435 **DNA Preparation**
436 Apoptosis constructs were synthesized from TWIST and transformed into DH5α cells for
437 amplification and plasmid purification. Condensate assay constructs were subcloned from
438 these synthesized constructs into vectors containing the appropriate chemically or light
439 inducible condensate elements. DNA was prepared using the QIAGEN Plasmid Plus Midi
440 Kit (Qiagen 12943) for transfection grade DNA purification. See supplemental methods
441 for additional details.
442 **Apoptosis assay**
443 200 μL of HT-1080 cells at to 7.5×10^4 cells per mL (15000 cells per well) were added to
444 each well of a microscope grade 96 well plate (Corning 3603). Plates were then
445 centrifuged at 330 rpm for 3 mins (Eppendorf, Centrifuge 5810). Plates were then
446 incubated at 37°C for 24 hours. Cells were then transfected with appropriate DNA
447 constructs with the lipofectamine 3000 kit (Thermo Fisher Scientific, L3000015) as
448 specified by the manufacturer. 24 hours after transfection, the transfection media was
449 removed and replaced with FluoroBrite DMEM Media (Thermo A1896702) supplemented

450 with 1x GlutaMAX (Thermo 35-050-061) and 10% FBS (Thermo Fisher Scientific,
451 10082147). This media also contained 13.2 μM (S)-(+)-Camptothecin (Sigma C9911-
452 100MG), 0.3 μM SiR-DNA stain (SpiroChrome CY-SC007), and 1.25 μM of the DEVD
453 peptide for detecting caspase activation (Sartorius 4440). The plates were sealed with
454 sterile Breathe-Easy film (USA scientific 9123-6100) and incubated at 37°C with 5% CO_2
455 for 30 minutes. After 30 min incubation, the plates were placed in an ImageXpress-
456 confocal plate imager with CO_2, humidity, and temperature control set to 37°C with 5%
457 CO_2 (Molecular Devices). Images of all wells were taken every 45 minutes and stored on
458 a remote server for later analysis. See supplemental methods for further details on this
459 method as well as the image analysis pipeline used.

460 **Confocal microscopy**

461 Confocal microscopy was done at the Nikon Imaging Center at Harvard Medical School
462 using a Nikon Ti fluorescence microscope attached to a Yokogawa W1 spinning disk
463 confocal. See supplemental methods for further details on the equipment and settings
464 used.

465 **Light inducible condensate assay**

466 HEK293-T cells were seeded on 96 well glass bottom plates from Cellvis (P96-1.5H-N).
467 Cells within each well were transfected with 50 ng of the LLPS1-iLID::EGFP::FTH1
468 (Addgene plasmid #122149) construct containing the core FTH1 scaffolding domain
469 attached to iLID for light inducible interactions. The cells were also transfected with 50 ng
470 of a construct containing the target protein attached to mCherry and SspB. The
471 transfection was allowed to continue overnight before the media was swapped to
472 FluoroBrite media supplemented with 10% FBS and 1x GlutaMAX. The cells were then

473 imaged using the settings listed above for mCherry and eGFP for the pre-induction
474 images. The cells were then exposed to 1 second of the DAPI imaging protocol described
475 in supplemental methods before new images were captured on the mCherry and eGFP
476 settings.

477 **Chemically inducible condensate assay**

478 HT-1080 cells were seeded on 96 well glass bottom plates from Cellvis (P96-1.5H-N).
479 Cells within each well were transfected with 50 ng of target construct fused to a mCherry-
480 2xFKBP domain. The transfection was allowed to continue overnight before the media
481 was swapped to FluoroBrite media supplemented with 10% FBS, 1x GlutaMAX, and 300
482 nM SiR-Hoechst. The cells were then imaged using the settings listed in the supplemental
483 methods for mCherry and SiR-Hoechst for the pre-induction images. Then, B/B dimerizer
484 (AP20187 ligand; TaKaRa 635058) was added to a final concentration of 500 nM in the
485 well. Imaging continued for 15 minutes with new images every 45 seconds.

486 **Caspase assay with chemically induced condensates**

487 These caspase assays are performed similarly to the standard caspase assays with a
488 few key differences. Briefly, HT-1080 cells were seeded as normal on to 96 well plates
489 and allowed to adhere overnight. The next day, 12.5 ng of nuclear mCherry marker and
490 37.5 ng of the target construct fused to mCherry-2xFKBP was transfected into the cells
491 as described above. The next day, 500 nM of the B/B dimerizer (TaKaRa 635058) was
492 added 2 hours before the start of the assay (or an Ethanol vehicle control was added).
493 The media was then removed and replaced with the apoptosis assay media described
494 above with the addition of 500 nM B/B dimerizer or a vehicle control. The rest of the assay
495 proceeded as normal.

496

497 **Abbreviations**

498 ExTol: extremotolerance-associated

499 IDP: Intrinsically Disordered Protein

500 LEA: Late Embryonic Abundant (protein)

501 ApoE: Apolipoprotein E

502 DHR: Designed helical repeat (protein)

503 CPT: Camptothecin

504 ATCC: American Type Culture Collection

505 XIAP: X-linked inhibitor of apoptosis

506 CAHS: Cytosolic Abundant Heat Soluble (protein)

507 FTH1: Ferritin Heavy Chain 1

508 iLID: light inducible dimer

509 SspB: Stringent Starvation Protein B

510 eGFP: Enhanced Green Fluorescent Protein

511 FKBP: FK506 binding protein

512 PvLEA: *Polypedilum vanderplanki* Late Embryonic Abundant (Protein)

513 MAPK: Mitogen-activated protein kinase

514 Apaf: Apoptotic protease activating factor

515 EMEM: Eagle's Minimum Essential Medium

516 FBS: Fetal bovine serum

517 DMEM: Dulbecco's Modified Eagle Medium

518

519 **Author Information.**

520 Correspondences should be sent to Pamela Silver, Harvard Medical School Department
521 of Systems Biology 200 Longwood Avenue Warren Alpert Building Boston, MA 02115.

522

523 **Author Contributions**

524 M.T.V. and D.T.N. designed and performed experiments, analyzed the data, and wrote
525 the paper. N.N.T. analyzed the data and wrote the paper. M.E.O provided technical
526 support. N.J.R., K.B.B., and N.P.B., designed constructs. D.B. and J.C.W. managed the
527 teams and provided key insight. D.S.M., R.L.C., and P.A.S., designed constructs,
528 managed teams, and wrote the paper.

529

530 **Acknowledgements**

531 Research was sponsored by the NSF, DARPA, the Wyss Institute for Biologically inspired
532 engineering, and the Army Research Office and was accomplished under Cooperative
533 Agreement Number W911NF-19-2-0017. M.T.V. was sponsored by the National Science
534 Foundation under Grant No. 2010370. D.T.N., N.N.T., M.E.O., N.J.R., K.P.B., J.C.W,
535 D.S.M., and P.A.S. were supported by the Harvard Medical School Department of
536 Systems Biology. J.C.W. was further supported by the Harvard Medical School
537 Laboratory of Systems Pharmacology. K.P.B. and D.S.M. were further supported by CZI
538 Neurodegenerative Challenge Ben Barres Early Career Award (CZI2018-191853). N.P.B
539 was further supported by the HHMI Hanna Gray fellowship (grant GT11817). We would
540 like to acknowledge Clarence Yapp for help with microscopy as well as the NCI U54-
541 CA225088 grant and a gift from the Ludwig Institute for Cancer Research to the

542 Laboratory for Systems Pharmacology. We would like to acknowledge the Nikon Imaging
543 Center at Harvard Medical Center for providing microscope support. The views and
544 conclusions contained in this document are those of the authors and should not be
545 interpreted as representing the official policies, either expressed or implied, of any funding
546 agency including the NSF, DARPA, the Army Research Office, or the U.S. Government.
547 The U.S. Government is authorized to reproduce and distribute reprints for Government
548 purposes notwithstanding any copyright notation herein.

549

550 **Bibliography & References**

551

552 1. Jonsson, K. I.; Rabbow, E.; Schill, R. O.; Harms-Ringdahl, M.; Rettberg, P., Tardigrades
553 survive exposure to space in low Earth orbit. *Curr Biol* **2008,** *18* (17), R729-R731.
554 2. Thevelein, J. M., Regulation of trehalose mobilization in fungi. *Microbiol Rev* **1984,** *48*
555 (1), 42-59.
556 3. Boothby, T. C.; Tapia, H.; Brozena, A. H.; Piszkiewicz, S.; Smith, A. E.; Giovannini, I.;
557 Rebecchi, L.; Pielak, G. J.; Koshland, D.; Goldstein, B., Tardigrades Use Intrinsically Disordered
558 Proteins to Survive Desiccation. *Mol Cell* **2017,** *65* (6), 975-984 e5.
559 4. Dijksterhuis, J.; Nijsse, J.; Hoekstra, F. A.; Golovina, E. A., High viscosity and anisotropy
560 characterize the cytoplasm of fungal dormant stress-resistant spores. *Eukaryot Cell* **2007,** *6* (2),
561 157-70.
562 5. Parry, B. R.; Surovtsev, I. V.; Cabeen, M. T.; O'Hern, C. S.; Dufresne, E. R.; Jacobs-Wagner,
563 C., The bacterial cytoplasm has glass-like properties and is fluidized by metabolic activity. *Cell*
564 **2014,** *156* (1-2), 183-94.
565 6. Hand, S. C.; Menze, M. A.; Toner, M.; Boswell, L.; Moore, D., LEA proteins during water
566 stress: not just for plants anymore. *Annu Rev Physiol* **2011,** *73*, 115-34.
567 7. Chakrabortee, S.; Meersman, F.; Kaminski Schierle, G. S.; Bertoncini, C. W.; McGee, B.;
568 Kaminski, C. F.; Tunnacliffe, A., Catalytic and chaperone-like functions in an intrinsically
569 disordered protein associated with desiccation tolerance. *Proc Natl Acad Sci U S A* **2010,** *107*
570 (37), 16084-9.
571 8. Belott, C.; Janis, B.; Menze, M. A., Liquid-liquid phase separation promotes animal
572 desiccation tolerance. *Proc Natl Acad Sci U S A* **2020,** *117* (44), 27676-27684.
573 9. Hyman, A. A.; Weber, C. A.; Julicher, F., Liquid-liquid phase separation in biology. *Annu*
574 *Rev Cell Dev Biol* **2014,** *30*, 39-58.
575 10. Shin, Y.; Brangwynne, C. P., Liquid phase condensation in cell physiology and disease.
576 *Science* **2017,** *357* (6357).
577 11. Boeynaems, S.; Alberti, S.; Fawzi, N. L.; Mittag, T.; Polymenidou, M.; Rousseau, F.;
578 Schymkowitz, J.; Shorter, J.; Wolozin, B.; Van Den Bosch, L.; Tompa, P.; Fuxreiter, M., Protein
579 Phase Separation: A New Phase in Cell Biology. *Trends Cell Biol* **2018,** *28* (6), 420-435.

580 12. Choi, J. M.; Holehouse, A. S.; Pappu, R. V., Physical Principles Underlying the Complex
581 Biology of Intracellular Phase Transitions. *Annu Rev Biophys* **2020,** *49*, 107-133.
582 13. Jiang, S.; Fagman, J. B.; Chen, C.; Alberti, S.; Liu, B., Protein phase separation and its role
583 in tumorigenesis. *Elife* **2020,** *9*.
584 14. Boija, A.; Klein, I. A.; Young, R. A., Biomolecular Condensates and Cancer. *Cancer Cell*
585 **2021,** *39* (2), 174-192.
586 15. Boija, A.; Klein, I. A.; Sabari, B. R.; Dall'Agnese, A.; Coffey, E. L.; Zamudio, A. V.; Li, C. H.;
587 Shrinivas, K.; Manteiga, J. C.; Hannett, N. M.; Abraham, B. J.; Afeyan, L. K.; Guo, Y. E.; Rimel, J.
588 K.; Fant, C. B.; Schuijers, J.; Lee, T. I.; Taatjes, D. J.; Young, R. A., Transcription Factors Activate
589 Genes through the Phase-Separation Capacity of Their Activation Domains. *Cell* **2018,** *175* (7),
590 1842-1855 e16.
591 16. Hubstenberger, A.; Courel, M.; Benard, M.; Souquere, S.; Ernoult-Lange, M.; Chouaib, R.;
592 Yi, Z.; Morlot, J. B.; Munier, A.; Fradet, M.; Daunesse, M.; Bertrand, E.; Pierron, G.;
593 Mozziconacci, J.; Kress, M.; Weil, D., P-Body Purification Reveals the Condensation of Repressed
594 mRNA Regulons. *Mol Cell* **2017,** *68* (1), 144-157 e5.
595 17. Tolleter, D.; Jaquinod, M.; Mangavel, C.; Passirani, C.; Saulnier, P.; Manon, S.; Teyssier,
596 E.; Payet, N.; Avelange-Macherel, M. H.; Macherel, D., Structure and function of a mitochondrial
597 late embryogenesis abundant protein are revealed by desiccation. *Plant Cell* **2007,** *19* (5), 1580-
598 9.
599 18. Leon, D., III, Occurrence of a Repeating 11-Mer Amino Acid Sequence Motif in Diverse
600 Organisms. *Protein & Peptide Letters* **2001,** *8* (2), 115-122.
601 19. Bussell, R., Jr.; Eliezer, D., A structural and functional role for 11-mer repeats in alpha-
602 synuclein and other exchangeable lipid binding proteins. *J Mol Biol* **2003,** *329* (4), 763-78.
603 20. Li, S.; Chakraborty, N.; Borcar, A.; Menze, M. A.; Toner, M.; Hand, S. C., Late
604 embryogenesis abundant proteins protect human hepatoma cells during acute desiccation.
605 *Proc Natl Acad Sci U S A* **2012,** *109* (51), 20859-64.
606 21. Tanaka, S.; Tanaka, J.; Miwa, Y.; Horikawa, D. D.; Katayama, T.; Arakawa, K.; Toyoda, A.;
607 Kubo, T.; Kunieda, T., Novel mitochondria-targeted heat-soluble proteins identified in the
608 anhydrobiotic Tardigrade improve osmotic tolerance of human cells. *PLoS One* **2015,** *10* (2),
609 e0118272.
610 22. Mertens, J.; Aliyu, H.; Cowan, D. A., LEA Proteins and the Evolution of the WHy Domain.
611 *Appl Environ Microbiol* **2018,** *84* (15).
612 23. Makarova, K. S.; Aravind, L.; Wolf, Y. I.; Tatusov, R. L.; Minton, K. W.; Koonin, E. V.; Daly,
613 M. J., Genome of the extremely radiation-resistant bacterium Deinococcus radiodurans viewed
614 from the perspective of comparative genomics. *Microbiol Mol Biol Rev* **2001,** *65* (1), 44-79.
615 24. Yamazaki, Y.; Zhao, N.; Caulfield, T. R.; Liu, C. C.; Bu, G., Apolipoprotein E and Alzheimer
616 disease: pathobiology and targeting strategies. *Nat Rev Neurol* **2019,** *15* (9), 501-518.
617 25. Erdos, G.; Dosztanyi, Z., Analyzing Protein Disorder with IUPred2A. *Curr Protoc*
618 *Bioinformatics* **2020,** *70* (1), e99.
619 26. Biegert, A.; Soding, J., De novo identification of highly diverged protein repeats by
620 probabilistic consistency. *Bioinformatics* **2008,** *24* (6), 807-14.
621 27. Eisenberg, D.; Weiss, R. M.; Terwilliger, T. C., The helical hydrophobic moment: a
622 measure of the amphiphilicity of a helix. *Nature* **1982,** *299* (5881), 371-4.

623 28. Furuki, T.; Niwa, T.; Taguchi, H.; Hatanaka, R.; Kikawada, T.; Sakurai, M., A LEA model
624 peptide protects the function of a red fluorescent protein in the dry state. *Biochem Biophys Rep*
625 **2019,** *17*, 27-31.
626 29. Brunette, T. J.; Parmeggiani, F.; Huang, P. S.; Bhabha, G.; Ekiert, D. C.; Tsutakawa, S. E.;
627 Hura, G. L.; Tainer, J. A.; Baker, D., Exploring the repeat protein universe through computational
628 protein design. *Nature* **2015,** *528* (7583), 580-4.
629 30. Li, F.; Jiang, T.; Li, Q.; Ling, X., Camptothecin (CPT) and its derivatives are known to target
630 topoisomerase I (Top1) as their mechanism of action: did we miss something in CPT analogue
631 molecular targets for treating human disease such as cancer? *Am J Cancer Res* **2017,** *7* (12),
632 2350-2394.
633 31. Wall, M. E.; Wani, M. C.; Cook, C. E.; Palmer, K. H.; McPhail, A. T.; Sim, G. A., Plant
634 Antitumor Agents. I. The Isolation and Structure of Camptothecin, a Novel Alkaloidal Leukemia
635 and Tumor Inhibitor from Camptotheca acuminata1,2. *Journal of the American Chemical Society*
636 **1966,** *88* (16), 3888-3890.
637 32. Bortner, C. D.; Cidlowski, J. A., Cellular mechanisms for the repression of apoptosis.
638 *Annu Rev Pharmacol Toxicol* **2002,** *42*, 259-81.
639 33. Rasheed, S.; Nelson-Rees, W. A.; Toth, E. M.; Arnstein, P.; Gardner, M. B.,
640 Characterization of a newly derived human sarcoma cell line (HT-1080). *Cancer* **1974,** *33* (4),
641 1027-33.
642 34. Obexer, P.; Ausserlechner, M. J., X-linked inhibitor of apoptosis protein - a critical death
643 resistance regulator and therapeutic target for personalized cancer therapy. *Front Oncol* **2014,**
644 *4*, 197.
645 35. Li, W.; Lee, M. K., Antiapoptotic property of human alpha-synuclein in neuronal cell lines
646 is associated with the inhibition of caspase-3 but not caspase-9 activity. *J Neurochem* **2005,** *93*
647 (6), 1542-50.
648 36. Geng, X.; Guo, J.; Zang, X.; Chang, C.; Shang, H.; Wei, H.; Xu, C., Proteomic analysis of
649 eleven tissues in the Chinese giant salamander (Andrias davidianus). *Sci Rep* **2019,** *9* (1), 16415.
650 37. Bracha, D.; Walls, M. T.; Brangwynne, C. P., Probing and engineering liquid-phase
651 organelles. *Nat Biotechnol* **2019,** *37* (12), 1435-1445.
652 38. Bracha, D.; Walls, M. T.; Wei, M. T.; Zhu, L.; Kurian, M.; Avalos, J. L.; Toettcher, J. E.;
653 Brangwynne, C. P., Mapping Local and Global Liquid Phase Behavior in Living Cells Using Photo-
654 Oligomerizable Seeds. *Cell* **2018,** *175* (6), 1467-1480 e13.
655 39. Stanton, B. Z.; Chory, E. J.; Crabtree, G. R., Chemically induced proximity in biology and
656 medicine. *Science* **2018,** *359* (6380).
657 40. Yagi-Utsumi, M.; Aoki, K.; Watanabe, H.; Song, C.; Nishimura, S.; Satoh, T.; Yanaka, S.;
658 Ganser, C.; Tanaka, S.; Schnapka, V.; Goh, E. W.; Furutani, Y.; Murata, K.; Uchihashi, T.; Arakawa,
659 K.; Kato, K., Desiccation-induced fibrous condensation of CAHS protein from an anhydrobiotic
660 tardigrade. *bioRxiv* **2021**, 2021.06.22.449423.
661 41. Arimoto, K.; Fukuda, H.; Imajoh-Ohmi, S.; Saito, H.; Takekawa, M., Formation of stress
662 granules inhibits apoptosis by suppressing stress-responsive MAPK pathways. *Nat Cell Biol*
663 **2008,** *10* (11), 1324-32.
664 42. Rao, P. N.; Reddy, K. S.; Bhuyan, A. K., Amyloid fibrillation of human Apaf-1 CARD.
665 *Biochemistry* **2009,** *48* (32), 7656-64.

666 43. Yasuda, S.; Tsuchiya, H.; Kaiho, A.; Guo, Q.; Ikeuchi, K.; Endo, A.; Arai, N.; Ohtake, F.;
667 Murata, S.; Inada, T.; Baumeister, W.; Fernandez-Busnadiego, R.; Tanaka, K.; Saeki, Y., Stress-
668 and ubiquitylation-dependent phase separation of the proteasome. *Nature* **2020,** *578* (7794),
669 296-300.
670 44. Gupta, I.; Singh, K.; Varshney, N. K.; Khan, S., Delineating Crosstalk Mechanisms of the
671 Ubiquitin Proteasome System That Regulate Apoptosis. *Front Cell Dev Biol* **2018,** *6*, 11.
672 45. Theillet, F. X.; Binolfi, A.; Frembgen-Kesner, T.; Hingorani, K.; Sarkar, M.; Kyne, C.; Li, C.;
673 Crowley, P. B.; Gierasch, L.; Pielak, G. J.; Elcock, A. H.; Gershenson, A.; Selenko, P.,
674 Physicochemical properties of cells and their effects on intrinsically disordered proteins (IDPs).
675 *Chem Rev* **2014,** *114* (13), 6661-714.
676 46. Lalli, G.; Schott, J. M.; Hardy, J.; De Strooper, B., Aducanumab: a new phase in
677 therapeutic development for Alzheimer's disease? *EMBO Mol Med* **2021,** *13* (8), e14781.
678 47. Hayashi, H.; Campenot, R. B.; Vance, D. E.; Vance, J. E., Protection of neurons from
679 apoptosis by apolipoprotein E-containing lipoproteins does not require lipoprotein uptake and
680 involves activation of phospholipase Cgamma1 and inhibition of calcineurin. *J Biol Chem* **2009,**
681 *284* (43), 29605-13.
682 48. Schellenberg, G. D.; D'Souza, I.; Poorkaj, P., The genetics of Alzheimer's disease. *Curr*
683 *Psychiatry Rep* **2000,** *2* (2), 158-64.
684